LA-UR-21-29598
Approved for public release; distribution is unlimited.

Title: Studying Rate of Fire Spread Using Landscape Statistics and FIRETEC

Author(s): Oliveto, Julia Andre
Jonko, Alexandra

Intended for: Report

Issued: 2021-09-28

Julia Oliveto

Florida State University Written Project Description

Studying Rate of Fire Spread Using Landscape Statistics and FIRETEC

Table of Contents:

Julia Oliveto

Florida State University Written Project Description

Abstract

Wildfires are multi-system and multi-scale processes that are influenced by the land and atmosphere. Here, we study the influence of land, in terms of topography and vegetation, on uphill and downhill fire spread using data of the state of California as a testbed. The California landscape is first quantified by reclassifying its dominant vegetation types into grass, trees, and shrubs. Next, statistics of slope, vegetation height, and live fuel moisture percentage for each dominant vegetation type are gathered to create ensembles of idealized computational fluid dynamics (CFD) model simulations representative of the landscape. Rate of spread values for each CFD simulation are recorded to observe the differences in perturbing slope and fuel moisture for each vegetation type. We have found that all vegetation types prefer slopes of less than 30 degrees. Trees in the California data are 10 to 40 meters high, whereas shrub heights are less than 3 meters and grass heights are less than 1 meter. The live fuel moisture percentage of both trees and shrubs fluctuates around approximately 100% over one year (2019-2020). Using these parameters as inputs into the CFD model, fire spread rate is found to be fastest in the grass ensemble (maximum 12 m s^{-1}), followed by shrubs (maximum 10 m s^{-1}) and lastly by trees (maximum 7 m s^{-1}). Increasing slope increases the spread rate of the uphill fire but the downhill spread decreases for slopes greater than 15 degrees. Increasing fuel moisture decreases the spread rate both up and down the hill. This study highlights the impacts that topography and vegetation have on fire spread.

Introduction

Topography and vegetation are two of the main drivers of fire behavior (Butler et al, 2007, Agee, 1996). Examples include ridge lines serving as natural barriers to fire progression or high intensity crown fires driven by the presence of dry trees (Sharples et al, 2012, Kuljian et al, 2010). One important topographic driver of fire behavior is the terrain slope. In the presence of wind and under identical fuel conditions, fire spread

increases with increasing slope as the angle of radiation between the flame front and the ground decreases (Butler et al, 2007). Fire behavior also changes seasonally depending on vegetation (e.g., fuel moisture) and atmospheric changes (e.g., regional weather events) (Bessie et al, 1995, Hess et al, 2001, Swetnam, 1993). Therefore, accurate characterizations of the landscape are needed to properly describe and predict fire behavior.

CFD models of coupled fire-atmosphere interactions, such as HIGRAD/FIRETEC (Linn et al, 2002), Wildland Urban Interface Fire Dynamics Simulator (WFDS), and Weather Research and Forecasting-Fire (WRF-Fire) can be used to provide detailed information of wildfire behavior under the effects of land and atmosphere (Sullivan, 2009). However, due to the high resolutions necessary for representing relevant processes, these models operate on limited spatial and short temporal scales. These CFD models are able to represent details of fire spread during a portion of an individual event and can offer information and insights about fire behavior over realistic terrains. They are not used however to simulate trends in fire behavior over long periods of time or across larger regions due to their high computational expenses. While such fine-scale CFD models cannot be implemented on a global scale, the data they generate can be used to inform representations of the aggregated macroscale influence of fires on the land surface and atmosphere. Here, we use HIGRAD/FIRETEC for this purpose. HIGRAD/FIRETEC is a 3-dimensional physics-based wildfire model which couples land-atmosphere-fire interactions on a scale of hundreds to thousands of meters (Linn et al, 1998). HIGRAD (High Gradient Flow Solver) is a computational atmospheric hydrodynamics model that represents airflow and its interaction with the terrain and vegetation (Reisner et al, 2000), while FIRETEC is a wildfire behavior model which represents combustion, heat transfer, aerodynamic drag, and turbulence (Linn et al, 2002). Together, HIGRAD/FIRETEC (abbreviated here as FIRETEC) represents fire behavior influenced by vegetation and atmosphere over complex terrain.

Julia Oliveto

Florida State University Written Project Description

This aims to study uphill and downhill fire spread based on FIRETEC simulations informed by terrain and vegetation data to investigate the effect landscape plays on fire behavior. Using the state of California as a testbed, a combination of geospatial datasets is analyzed that includes elevation, vegetation characteristics, and live fuel moisture content. Based on the landscape statistics obtained from these data, we create ensembles of fine-scale FIRETEC simulations for three super-sets of vegetation types (grasses, shrubs, trees). For each vegetation super-set, we then vary slope, wind speed, and fuel moisture. For each simulation, two rates of fire spread are calculated: an uphill rate of spread (ROS), and a downhill ROS. The ROS matrix obtained by this analysis highlights the effect terrain and vegetation have on fire behavior.

Methods

2.1 Characterizing the Landscape of California

We characterize the landscape across the state of California using several different datasets of topography and vegetation characteristics. For *topography*, we use elevation data from the US Geological Survey (USGS) National Elevation Dataset (NED) (U.S. Geological Survey, 2019). The ⅓ arc-second Digital Elevation Model (DEM) gives elevation at 30-m resolution and is created using remote sensing (Figure 1A). For *vegetation*, we use Landscape Fire and Resource Management Planning Tools (LANDFIRE), which is a collection of datasets describing vegetation, fuel, and topography of the entire US in 30-m resolution. LANDFIRE datasets are created using a combination of remote sensing and vegetation modeling (LANDFIRE, 2016) (Figure 1B). We obtain both topography and vegetation data for 62 1-degree by 1-degree tiles covering the state of California. The tiles are approximately 130 km by 110 km, though the exact size of each tile depends on latitude.

2.1.1 Vegetation data

For vegetation, we use a combination of LANDFIRE Existing Vegetation Type (EVT) and Existing Vegetation Height (EVH), both from the 2016 LANDFIRE product

(LANDFIRE, 2016).To simplify producing inputs for FIRETEC, we first reclassify the 21 EVTs into four supersets including trees, shrubs, grass, and non-burnable areas (Figure 2).

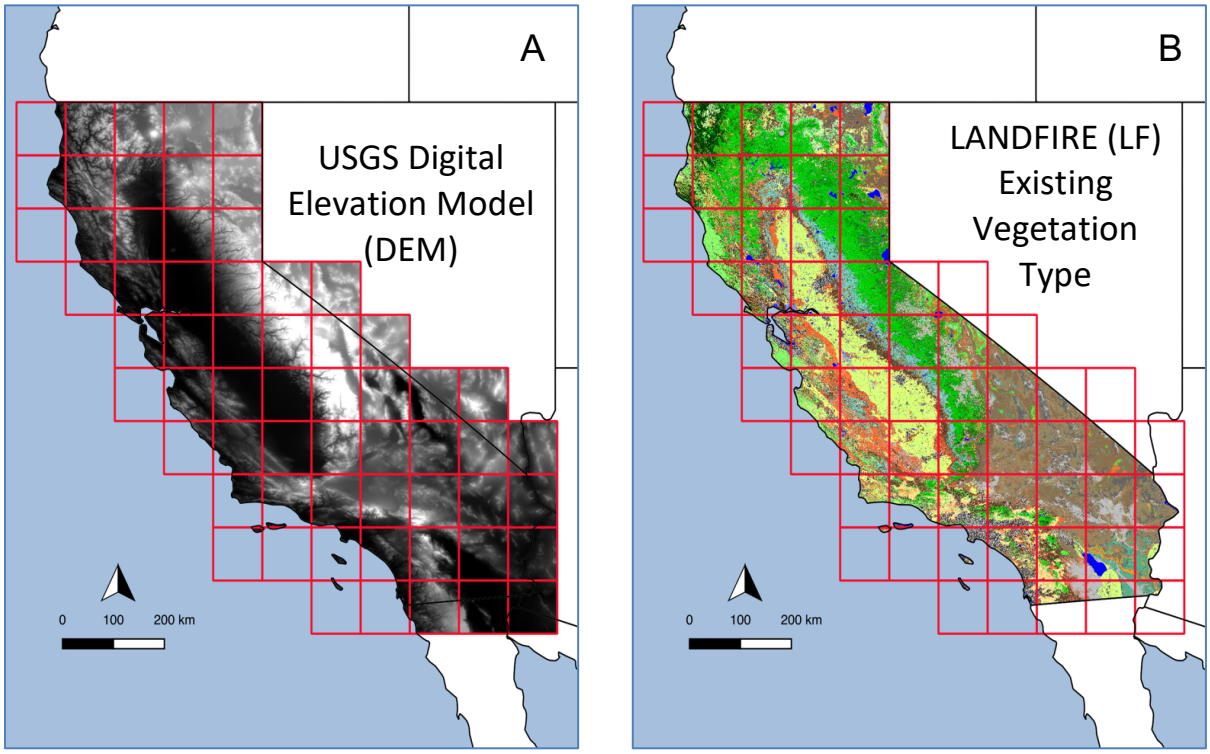

Figure 1 A: USGS Digital Elevation Model 30-m resolution 1 degree by 1 degree tiles covering California (left). B: LANDFIRE Existing Vegetation Type 30-m resolution 1 degree by 1 degree tiles covering California (right).

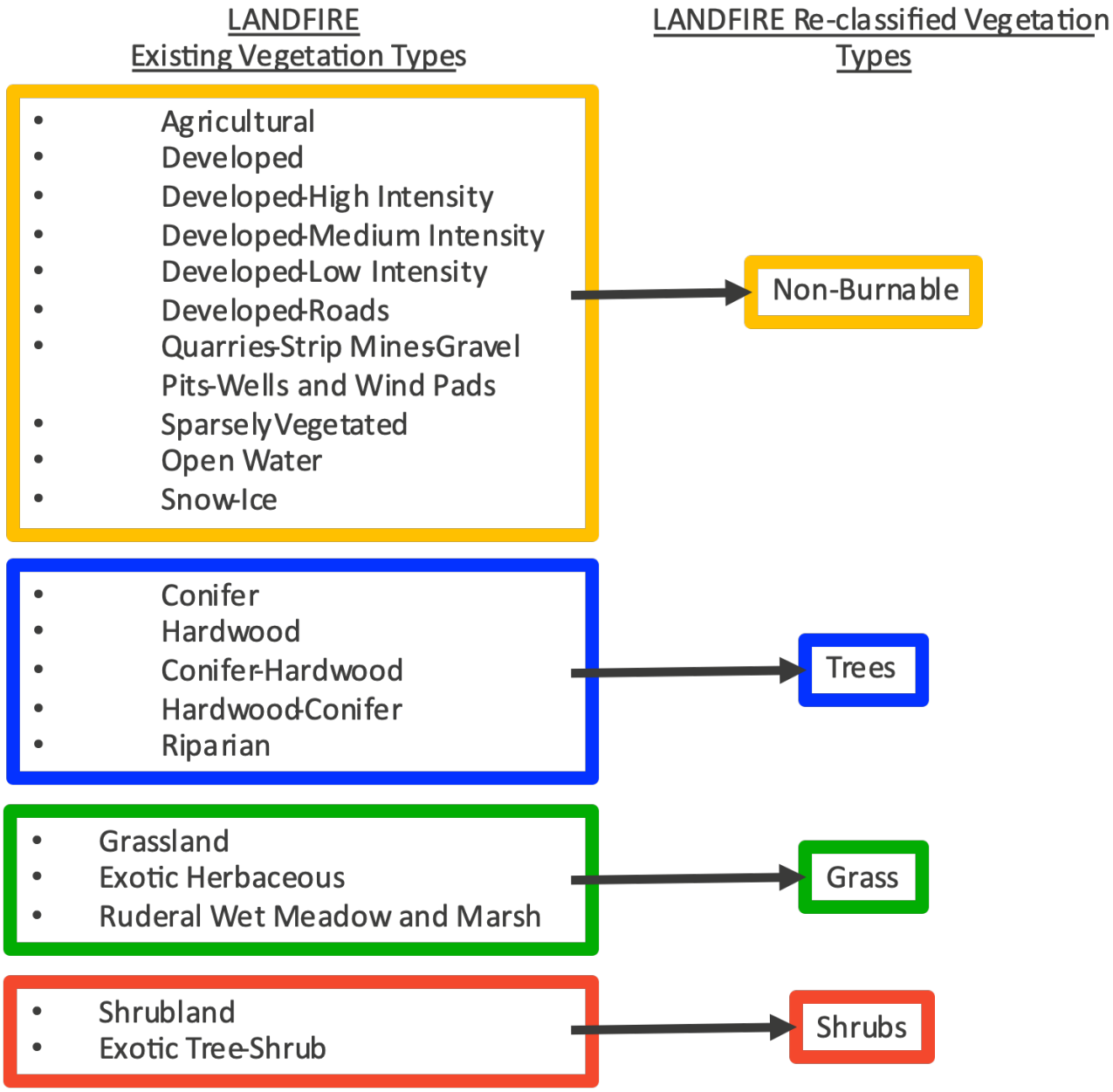

Figure 2 LANDFIRE Existing Vegetation Types and their reclassifications. A total of 21 vegetation types are reclassified into 4 vegetation types

The three burnable types (trees, grass, and shrubs) and their landscape statistics are the focus of the FIRETEC inputs. In addition to vegetation type, FIRETEC inputs needed to build fuel beds include information about the fuel structure such as: fuel

height for surface and canopy fuels, height to live crown (height from ground to canopy bottom), crown radius for shrubs and trees, fuel density, and fuel moisture. We obtain information about fuel heights from the LANDFIRE EVH variable. EVH is defined as “the average height of the dominant vegetation for a 30-m cell” (LANDFIRE, 2016). Figure 3 illustrates the LANDFIRE height of each reclassified vegetation type.

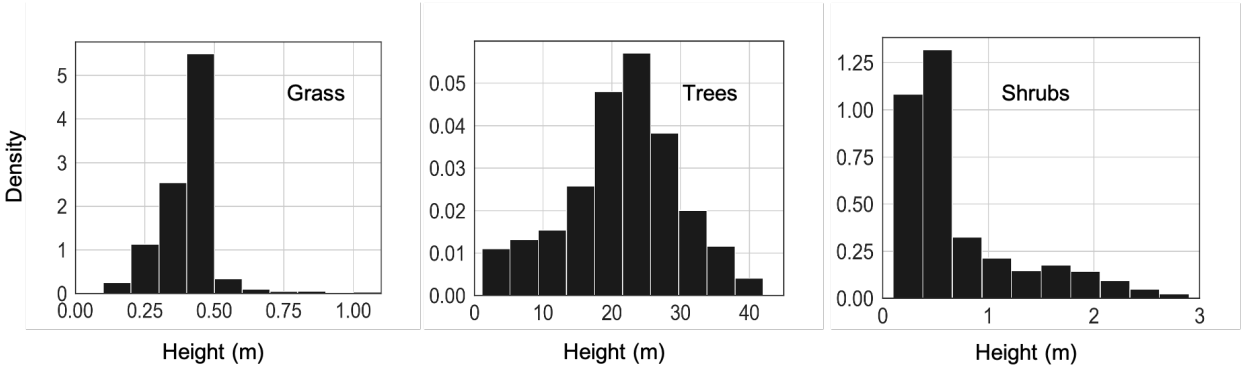

Figure 3 LANDFIRE height (m) of reclassified vegetation over the entire state of California

Figure 3 indicates that the grass heights range from 0 - 1 m with the highest density at 0.2 - 0.4 m. Tree height represents a normal distribution ranging from 0-40 m with a mean of 20 m. Short (<10 m) tree heights have a higher probability density than tall trees (>30 m). Based on these height distributions, we extract height to live crown and crown radius information from a dataset of 4,537 individual tree measurements taken near Blodgett Forest Research Station in CA, provided by Lucas Wells (personal communication, L. Wells, 03/06/2021). Shrub height is distributed with mean ~0.4 m, however heights of up to 3 m are represented in the data. A dataset from USFS (Li et al, 2016) is used containing 9 shrubs (chamise and manzanita) with breast diameter, tree height, and height to live crown defined.

Our bulk density values are a single FIRETEC input. Our grass bulk density is set to 0.5 kg m^{-3}, trees are 0.6 kg m^{-3}, and finally shrubs are 1.3 kg m^{-3}. To determine the amount of trees and shrubs necessary for the FIRETEC ensembles, we use LANDFIRE’s Existing Vegetation Cover (EVC) defined as “the vertically projected

percent cover of the live canopy layer for a 30-m cell" (LANDFIRE, 2016). The mean EVC percentage for trees is 49% and for shrubs is 23%. We use these values when creating the FIRETEC domains for trees and shrubs by randomly placing our vegetation and calculating the amount of fuel above the surface.

We vary surface fuel moisture for all three fuel types between 5% and 50 %, using a total of 5 surface fuel moisture values: 5%, 10%, 15%, 25%, 50%. For shrub and tree fuels, we set canopy fuel moisture to 100% in all simulations. This is because fire spread is most sensitive to variation in surface fuels, which can drive a fire spread even if fire does not affect the canopy (Mutlu et al, 2008). The choice of 100% canopy fuel moisture was made by considering the Live Fuel Moisture Content, defined as "the mass of water per unit dry biomass in vegetation", from Rao et al (2020). This is a dataset created from a combination of observations, satellite imagery, and machine learning, and is available at 250 m resolution for the western U.S. for the time period of 2016 to 2020. To gain an understanding of typical canopy fuel moistures in CA forests and shrublands, we evaluate LFMC values from 9/2019 to 8/2020 (LFMC dataset year) for each LANDFIRE reclassified type, downscale from 250 m to 30 m resolution. The LFMC dataset year is used because of the completeness of the data record over CA and its similar time frame to the 2016 LANDFIRE data. Figure 4 A and B first show LFMC histograms for trees and shrubs for the LFMC dataset year over CA. The 75th and 95th percentile of the data is denoted by the red dotted line. Figure 4 C and D next show the monthly trend of LFMC for trees and shrubs. The highlighted markers in the monthly graph represent the mean LFMC for the month with the error bars representing 1 standard deviation. Grey markers represent a sample of raw data points.

Julia Oliveto

Florida State University Written Project Description

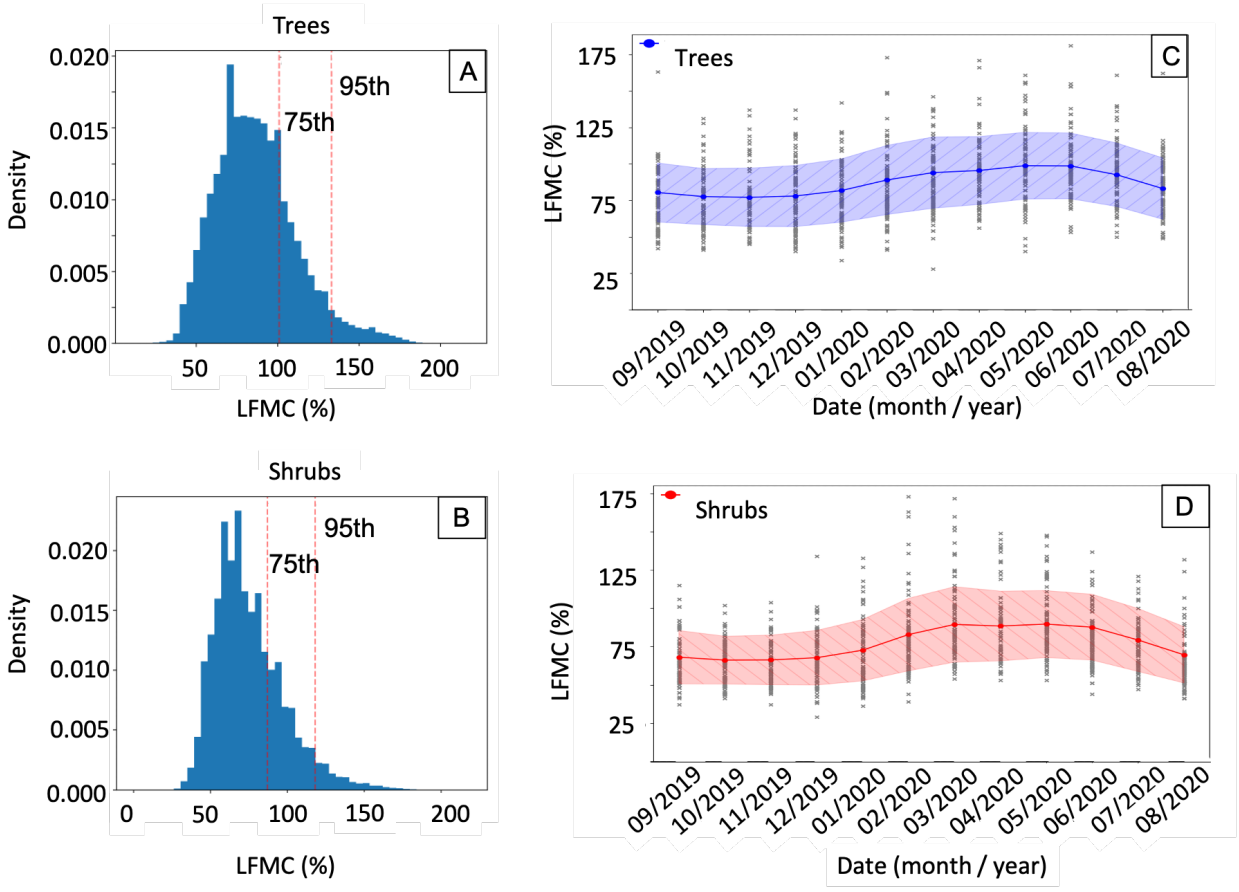

Figure 4 LFMC of CA reclassified vegetation types trees and shrubs during 9/2019 to 8/2020 (LFMC dataset year). A: Histograms of trees LFMC over CA; B: Histograms of shrubs LFMC over CA; C: Trees LFMC variations for each month over the data year; D: Shrubs LFMC variations for each month over the data year

Monthly LFMC of both vegetation types during the dataset year decrease from May to August and increase from December to March (Figure 4 C and D). LFMC in trees ranges from 75-95% +/- 20%. Shrub LFMC is lower than that for trees and ranges from 70-80% +/-17%. Based on this data and the fluctuations in LFMC over the dataset year, 100% LFMC is used for the canopy fuels in tree and shrub simulations.

2.1.2 Topography Data

To characterize topography, we convert USGS DEM elevations, $h(x, y)$, to local slope using the following equation:

$$Local\ Slope = S = arctan\ (\ \sqrt{(\partial_x h)^2 + (\partial_y h)^2}\ )$$

We then classify slope by vegetation type. Figure 5 shows histograms of local slope for each vegetation type. We use these distributions to determine slope ranges to use in FIRETEC simulations.

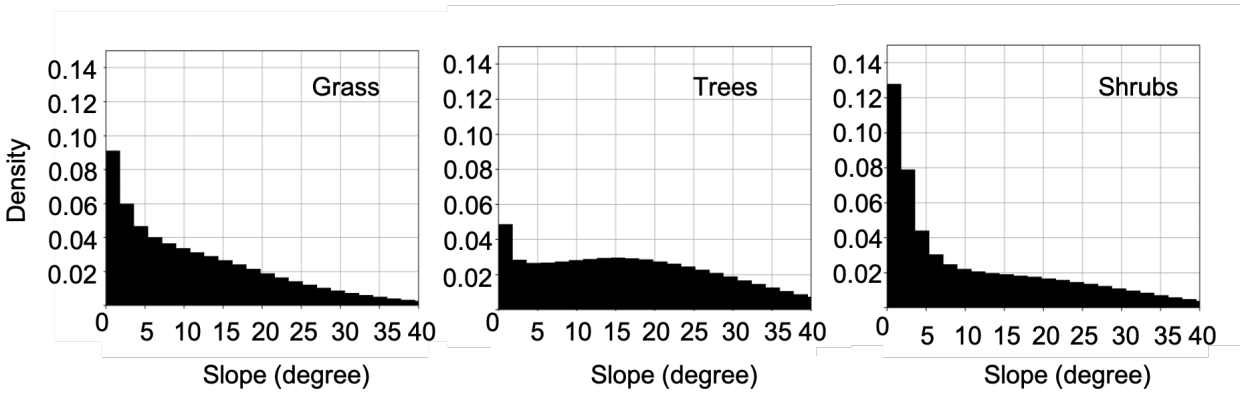

Figure 5 Slope histograms from DEM separated by burnable reclassified LANDFIRE vegetation types for all CA

Local slope distributions for each re-classified LANDFIRE type show a high frequency of slopes < 20 degrees in grass and shrubs. Steeper slopes are more prevalent in the tree superset. Based on this information, we build FIRETEC simulation domains spanning slopes (1-10, 15, 20, 30 degrees) which cover a broad range of the slope distributions presented above.

2.2 Creating a Fire Spread Response Matrix

We run FIRETEC to simulate fire spread through fuel beds created based on the vegetation and topography data described above. We use a domain with dimensions of 1000 m in x-direction, 600 m in y-direction, and 1200 m in z-direction. The domain

includes a hill with 13 different slopes (1-10, 15, 20, and 30 degrees). A schematic of the general simulation domain is shown in Figure 6.

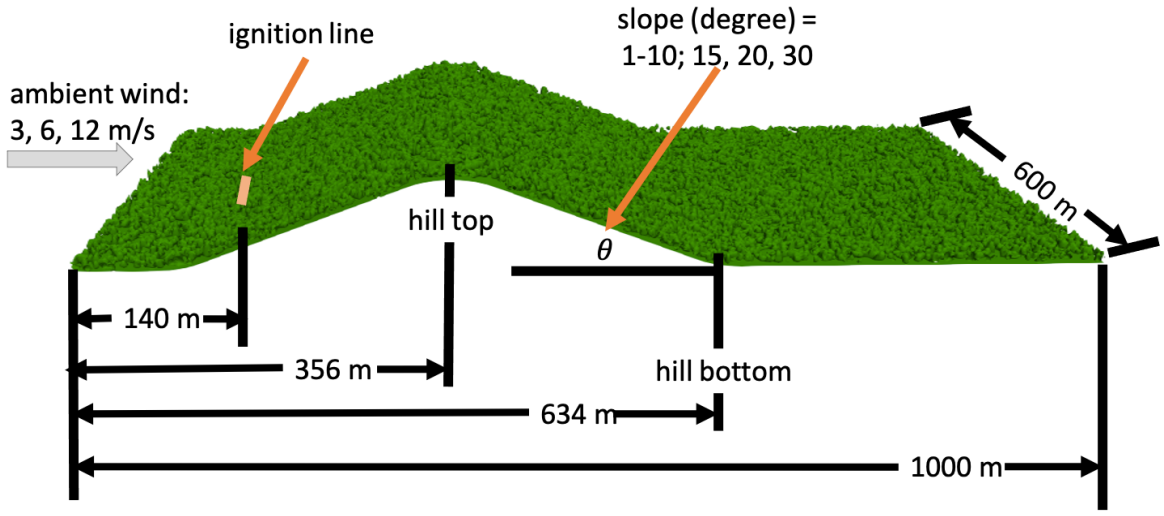

Figure 6 FIRETEC domain and simulation setup

The incline starts at 78 m from the inlet to the left. Between 122 meters and 316 meters from the inlet, the slope is uphill and constant. At 317 meters, the slope begins to curve. The top is located at 356 m. From there the hill is mirrored, with another section of constant slope between 398 m and 592 m from the inlet. Past 634 m from the inlet, and until the far end of the domain, the terrain is flat. The fire ignition line is parallel to the hill and located between 140 m from the inlet at the bottom of the constant slope uphill section of the hill. The ignition line is centered on the y-axis, is 2 m wide and 60 m long. We have tested several ignition line lengths, and have chosen 60 m to ensure that the domain boundaries do not interact with the simulated physics at least during uphill fire spread. Due to vorticity-driven lateral spread (see Section 4), the domain boundaries do interact with the fire on the downhill portion of the hill.

We initialize the wind field with a logarithmic profile for the wind in the *x*-direction (*u*) that is empirically defined based on LAI and vegetation height (Kaimal & Finnigan, 1994; Raupach et al., 1996). We use three different wind speeds to initialize FIRETEC

simulations. The streamwise velocity, u, is set to be equal to 3 m s^{-1}, 6 m s^{-1}, and 12 m s^{-1}, respectively, roughly 10 m above the canopy - or at 10 m for grass fuels, 45 m for trees, and 10 m for shrubs. At $t = t_0$ we assume that cross-stream and vertical velocities, v and w, are zero everywhere. The atmospheric stratification in all simulations is neutral, with an initial ambient temperature of 300 K.

FIRETEC fuel beds are created using vegetation inputs discussed above. We set up three simulation ensembles for the three reclassified fuel types, grass, shrub, and trees. The grass ensemble uses a fuel height of 0.3 m and a bulk fuel density of 0.5 kg m^{-3} for all simulations. Five surface fuel moisture values (5%, 10%, 15%, 25%, 50%) are chosen based on grass moistures from the Standard Fire Behavior Fuel Models (Scott et al, 2005). These grass fuel inputs are combined with 13 slopes and 3 wind speeds to result in 195 total FIRETEC simulations in grass fuels. To build the tree fuel beds, we first obtain a range of heights (10- 40 m) and most common species (douglas fir, ponderosa pine, sugar fir, & white birch) from LANDFIRE data. Next, we extract a subset of tree measurements, which match these parameters from Lucas Wells' Blodgett dataset. Values of tree height, height to live crown (height from ground to canopy bottom), and crown radius are used to build trees for FIRETEC, which are randomly distributed across the domain until the canopy bulk density in the domain equals 0.6 kg m^{-3}. Canopy fuel moisture for both trees and shrubs is held at 100% while surface fuel moisture is varied between 5% and 50%. Shrub fuel beds for FIRETEC simulations are set up in a similar way to trees instead using observational shrub measurements from Li et al. The canopy bulk density input for FIRETEC is set to 1.3 kg m^{-3}. Tree and shrub fuel inputs are again combined with 13 slopes and 3 wind speeds to result in 195 FIRETEC simulations each for tree and shrub fuels.

The speed of a fire in a FIRETEC simulation is measured as the rate of spread (ROS) defined here as the average speed of the fire across a 100m distance on the uphill and downhill constant slope portions of the FIRETEC domain (Figure 7).

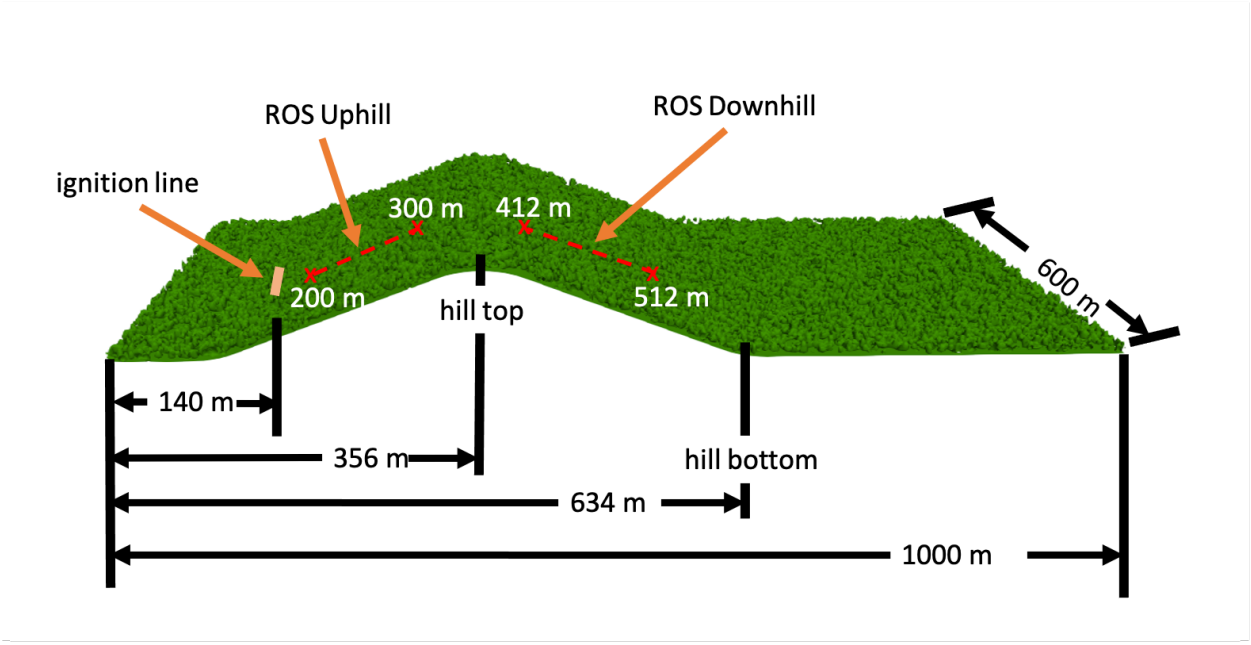

Figure 7 FIRETEC Domain with rate of spread (ROS) uphill and downhill portions defined

The placement of the 100 m segments is chosen because of the constant slope and adequate distance from the ignition line, which ensures that the fire line can develop before ROS is calculated.

Results

We obtain fire spread rate (ROS) from ensembles of FIRETEC simulations with varying slope, ambient wind speed, and surface fuel moisture for each re-classified burnable LANDFIRE type. These simulations represent a wildland fire moving through the domain. FIRETEC simulations for trees, grass, and shrubs all implement the same general domain (Figure 6). The domain size, ignition starting location, and ignition length are constant across all simulations, as well as the range of slope and ambient wind. The results of the FIRETEC simulations are recorded as the ROS up and down a constant sloped portion of the hill domain (Figure 7). Results for each vegetation type form a response matrix which highlights the difference in fire spread for varying

vegetation types and slopes (Figures 8-13). Simulations with no ROS recorded are yet to be completed.

3.1 Rate of Spread for Grass Simulation Ensembles

In the case of 3 m s^{-1} wind, uphill fire ROS generally increases with slope and decreases with fuel moistures 5%-50%. We see a decrease in ROS between slopes 9 and 10 degrees for all fuel moistures. There is no uphill spread for 50% fuel moisture at any slope. The two fastest ROS in this wind case, 3.4 and 3.3 m s^{-1}, occur on the 30-degree slope with 10% and 5% fuel moisture. For 6 m s^{-1} winds, a similar trend is seen with uphill fire ROS increasing with slope and decreasing with fuel moisture in all cases. The two fastest ROS in this wind case, 9.5 and 9.2 m s^{-1}, occur on the 30-degree slope with 10% and 5% fuel moisture. We again see a decrease in ROS between slopes 9 and 10 degrees for all fuel moistures. In the case of 12 m s^{-1} wind, the uphill ROS increases with slope and decreases with fuel moisture. The fastest ROS in the uphill case is 11.9 m s^{-1} at 5% fuel moisture (Figure 8).

For 3 m s^{-1} wind, the downhill ROS is zero for almost all fuel moistures greater than 5%. The 5% fuel moisture case shows downhill ROS between 0.2-0.4 m s^{-1} for slopes 1 to 9 degrees. Steeper slopes for this fuel moisture case show no ROS. The fire does not spread uphill or downhill in the 50% fuel moisture case. In the 6 m s^{-1} wind case, the downhill ROS for fuel moistures 5% and 10% increases with slope up to 15 degrees then decrease for cases of slope greater than 15 degrees. For 15%, 25%, and 50% fuel moistures, ROS decreases with increasing fuel moisture and fluctuates +/- 0.3 m s^{-1} for slopes 1 to 9 degrees. The fire does not spread downhill for slope 30 degrees and fuel moisture 5%, 10%, 15%, 25%, and 50%. For wind 12 m s^{-1}, the downhill ROS increases with slope until 15 degrees then decreases to speeds slower than the low slope cases with the same fuel moisture. The fire does not spread downhill for slope 30 degrees and fuel moisture 5%, 10%, 15%, 25% (Figure 9).

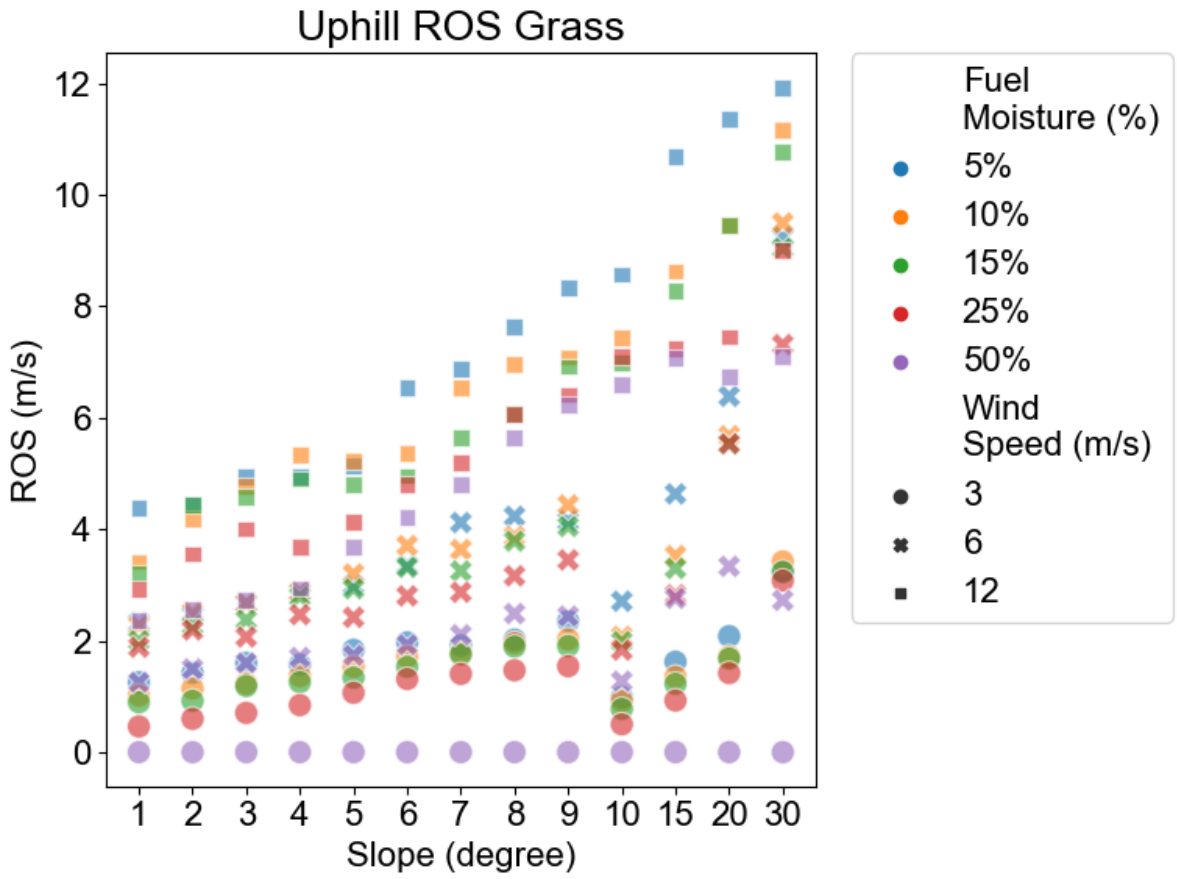

Figure 8 FIRETEC uphill ROS results for grass varying fuel moisture (5%: blue, 10%: orange, 15%: green, 25%: red, 50%: purple), and slope (1-10, 15, 20, 30 degrees). Initial wind speeds are denoted by symbols circle (3 m s^{-1}), cross (6 m s^{-1}), and square (12 m s^{-1}).

Julia Oliveto

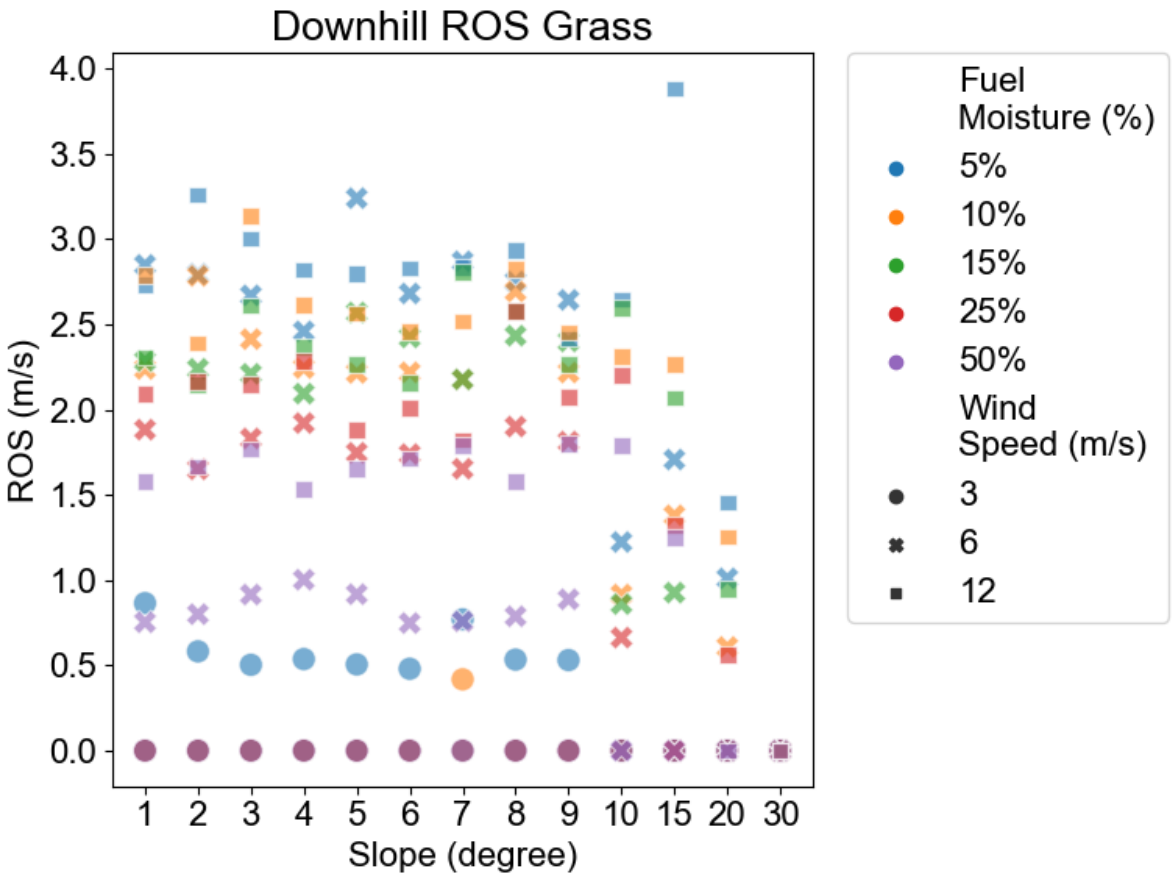

Figure 9 FIRETEC downhill ROS results for grass varying fuel moisture (5%: blue, 10%: orange, 15%: green, 25%: red, 50%: purple), and slope (1-10, 15, 20, 30 degrees). Initial wind speeds are denoted by symbols circle (3 m s^{-1}), cross (6 m s^{-1}), and square (12 m s^{-1}).

3.2 Rate of Spread for Tree Simulation Ensembles

For 3 m s^{-1} winds, uphill fire ROS is zero in almost all cases except for slope of 30 degrees and surface fuel moistures 5%, 10%, 15%, and 25%, and slope 20 degrees with fuel moisture 5%. These non-zero ROS decrease with increasing fuel moistures. The fastest ROS in this wind case, 1.8 m s^{-1}, occurs on the 30 degree slope at 5% fuel moisture. In the case of 6 m s^{-1} wind, ROS is zero for slopes 1 to 10 degrees and fuel moistures 10%-50% with the exception of 7 and 10 degree slopes at 10% fuel moisture. ROS increases with slope in the 5% fuel moisture case. The maximum ROS in this wind case is 5.3 m s^{-1} and occurs at 30 degree slope, 5% fuel moisture. In the case of 12 m s^{-1} wind, a similar trend is seen as in the grass cases with uphill fire ROS increasing with slope and decreasing with fuel moisture. There is no uphill spread in the 50% fuel moisture case. The fastest ROS in this wind case (and tree ensemble), 6.9 m s^{-1}, occurs on the 20 degree slope with 5% fuel moisture (Figure 10).

For 3 m s^{-1} winds, the downhill fire ROS is zero in all cases. In the case of 6 m s^{-1} wind, the downhill ROS is zero in most cases, with the exception of fuel moisture 5%, 10%, 15%, 25% and slopes 10, 15, 20, 30 degrees. No spread downhill is seen in the 50% fuel moisture case for any slope. In the case of 12 m s^{-1} wind, the non-zero downhill ROS values increase with slope and decrease with fuel moisture. No spread downhill is seen in the 50% fuel moisture case (Figure 11).

Julia Oliveto

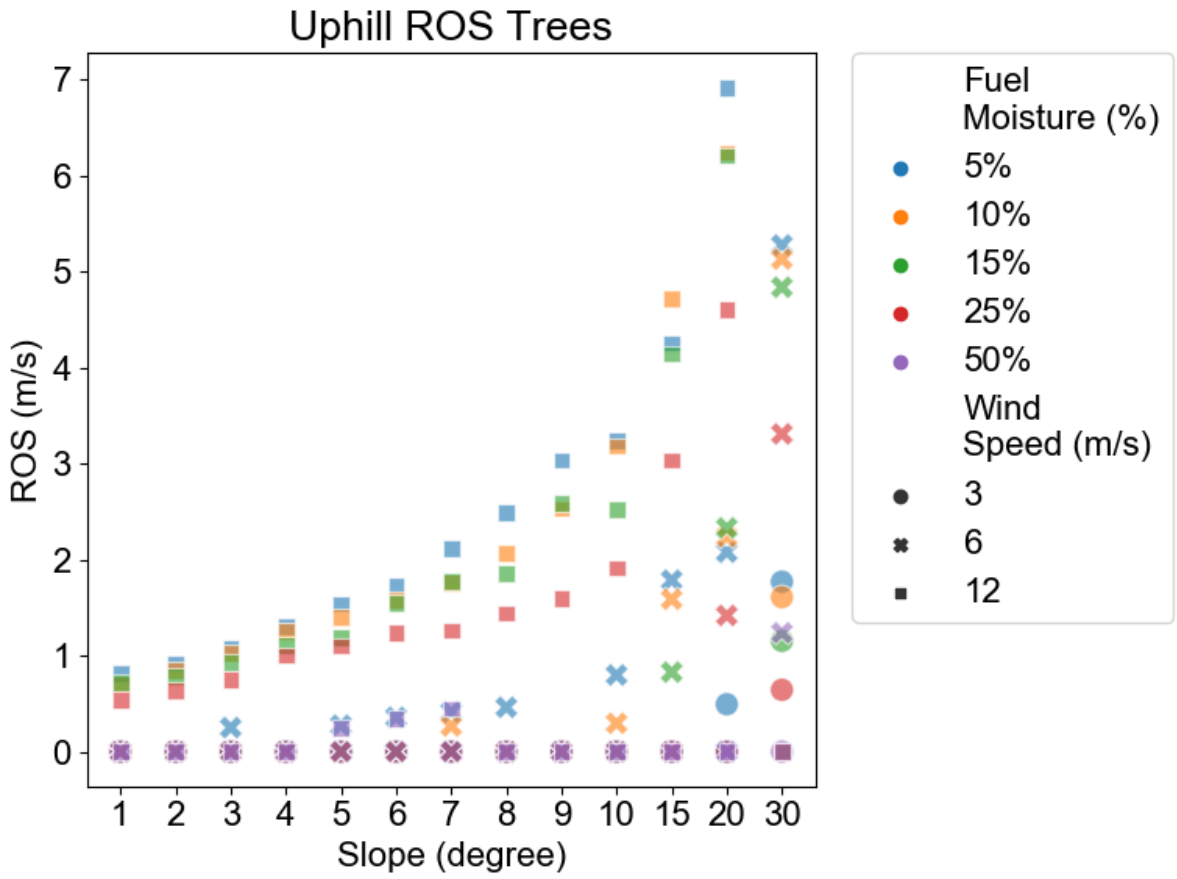

Figure 10 FIRETEC uphill ROS results for trees varying fuel moisture (5%: blue, 10%: orange, 15%: green, 25%: red, 50%: purple), and slope (1-10, 15, 20, 30 degrees). Initial wind speeds are denoted by symbols circle (3 m s^{-1}), cross (6 m s^{-1}), and square (12 m s^{-1}).

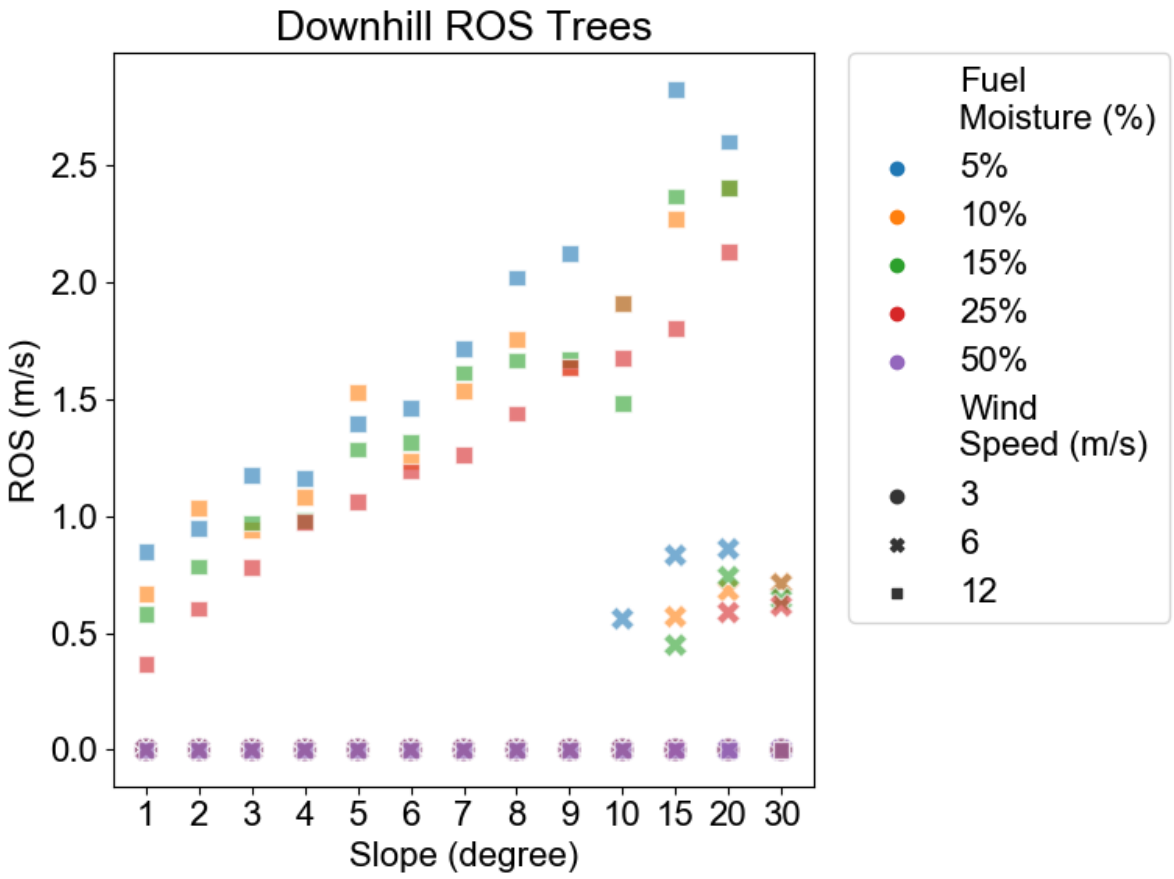

Figure 11 FIRETEC downhill ROS results for trees varying fuel moisture (5%: blue, 10%: orange, 15%: green, 25%: red, 50%: purple), and slope (1-10, 15, 20, 30 degrees). Initial wind speeds are denoted by symbols circle (3 m s^{-1}), cross (6 m s^{-1}), and square (12 m s^{-1}).

3.3 Rate of Spread for Shrub Simulation Ensembles

For 3 m s^{-1} wind, uphill fire ROS increases with slope and decreases with fuel moisture. The fastest ROS value, 2.5 m s^{-1}, occurs at 30-degree slope and fuel moistures 5% and 10%. No uphill spread is seen for slope 1 to 7 degrees at 15% and 25% fuel moisture. In the case of 6 m s^{-1} wind, uphill fire ROS increases with slope and decreases with fuel moisture. We see non-zero ROS values for all uphill fires at all fuel moistures and slope, with the maximum (4.7 m s^{-1}) occurring at 30 degree slope, 5% fuel moisture. In the case of 12 m s^{-1} wind, the uphill ROS again increases with slope and decreases with fuel moisture. Uphill spread is seen in all fuel moisture cases with maximum 10.3 m s^{-1} occurring at 30 degree slope, 5% fuel moisture (Figure 12).

In the case of 3 m s^{-1} wind, the downhill ROS is zero for all slope and fuel moisture cases. For 6 m s^{-1} wind, the downhill ROS increases with slope until 15% then decreases for cases slope 20, 30 degrees. No downhill ROS is seen for 20 or 30 degree slope in any fuel moisture case. In the case of 12 m s^{-1} wind, the downhill ROS increases with slope until 15 degrees then decreases to speeds comparable to the low slope cases in their same fuel moisture column. Downhill spread is seen in all fuel moisture cases except slope 30 degrees (Figure 13).

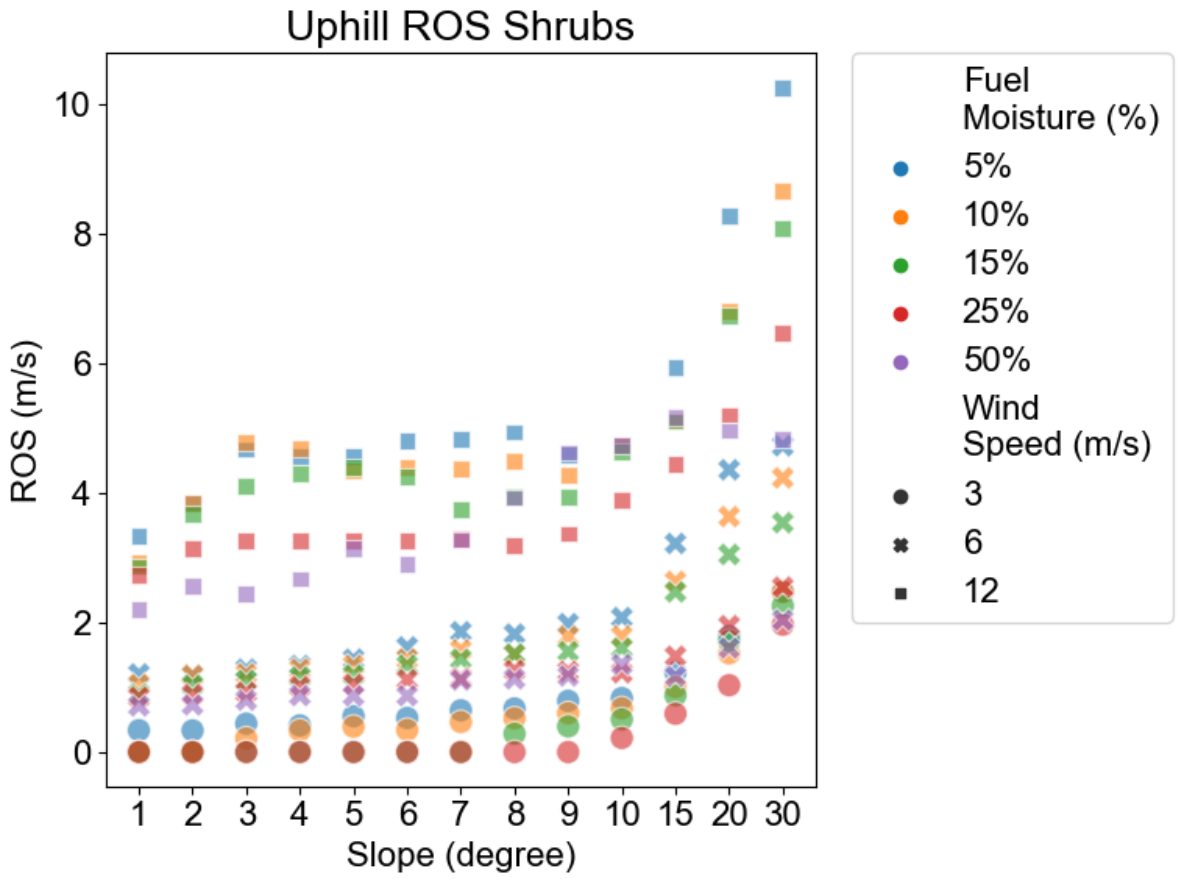

Figure 12 FIRETEC uphill ROS results for shrubs varying fuel moisture (5%: blue, 10%: orange, 15%: green, 25%: red, 50%: purple), and slope (1-10, 15, 20, 30 degrees). Initial wind speeds are denoted by symbols circle (3 m s^{-1}), cross (6 m s^{-1}), and square (12 m s^{-1}).

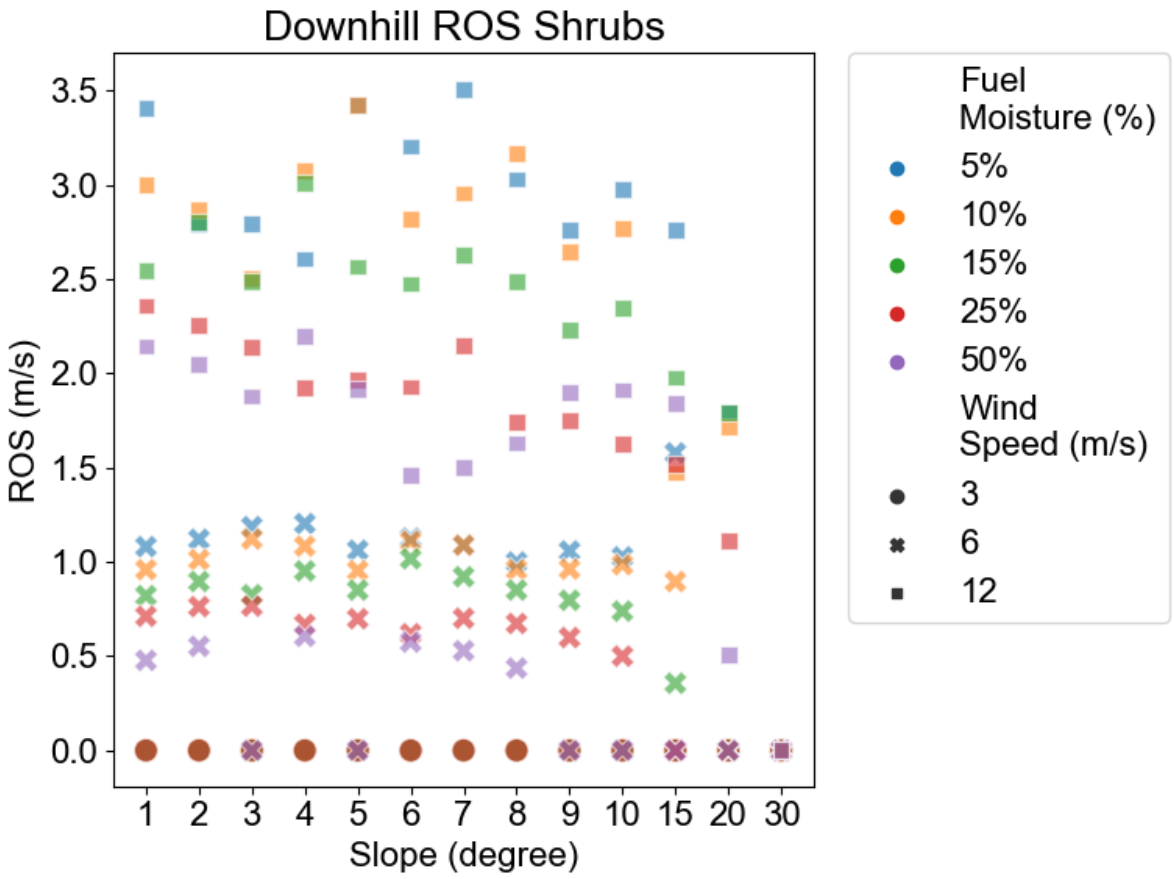

Figure 13 FIRETEC uphill ROS results for shrubs varying fuel moisture (5%: blue, 10%: orange, 15%: green, 25%: red, 50%: purple), and slope (1-10, 15, 20, 30 degrees). Initial wind speeds are denoted by symbols circle (3 m s^{-1}), cross (6 m s^{-1}), and square (12 m s^{-1}).

Conclusion

In the analysis of the CA landscape using LANDFIRE vegetation, USGS elevation, and Rao et al. LFMC data sets, we find differences in the statistics of the three burnable fuel types: trees, grass, and shrubs. Grass and shrubs show a preference for slopes < 10 degrees, whereas trees are found on steeper slopes between 10 - 30 degrees as well. LFMC shows similar ranges for trees and shrubs, however, on average tree LFMC is higher than for shrubs.

Based on these data, representative FIRETEC simulations are created using slopes ranging from 1-30 degrees, vegetation heights consistent with the analysis, surface fuel moisture ranging 5-50%, and tree and shrub canopy LFMCs at 100%. Ensembles are run for three different mean wind speeds: 3 m s^{-1} , 6 m s^{-1}, and 12 m s^{-1}. The FIRETEC simulations highlight how changing slope, vegetation type, wind speed, and fuel moisture affect fire spread. For each vegetation type, increasing slope or wind speed also increases the uphill spread rate. The downhill spread fluctuates and the trends are not as straightforward as in the uphill cases. For a majority of the simulations, however, downhill spread decreases with slope and at the steepest slope values shows no spread. Increasing fuel moisture decreases the uphill and downhill ROS. It is likely that downhill fire spread is impacted by vorticity-driven lateral spread (VLS) in our simulations. This mechanism affects fires spreading across ridge-tops, where vortex interactions with the terrain induces fire spread perpendicular to the wind direction on lee slopes, rather than downhill fire spread (Raposo et al, 2015, Sharples et al, 2012).

Comparing fire spread across vegetation types, we find that grass fuels feature the fastest ROS values. One reason is that these simulations have no canopy cover and thus the wind can flow unimpeded. The next fastest ROS values are shrubs which had uphill spread rates similar to the grass ensemble. The slowest ROS values came from the tree ensemble which also had several instances of no fire spread, especially in the slow wind case. This study highlights the effects topography and vegetation characteristics have on wildfire spread.

References

Agee, J. K. (1996, January). The influence of forest structure on fire behavior. In Proceedings of the 17th annual forest vegetation management conference (pp. 52-68).

Arora, V. K., & Boer, G. J. (2005). Fire as an interactive component of dynamic vegetation models. Journal of Geophysical Research: Biogeosciences, 110(G2), n/a. https://doi.org/10.1029/2005jg000042

Bessie, W. C., & Johnson, E. A. (1995). The Relative Importance of Fuels and Weather on Fire Behavior in Subalpine Forests. Ecology, 76(3), 747–762. https://doi.org/10.2307/1939341

Bond-lamberty, B., Peckham, S. D., Gower, S. T., & Ewers, B. E. (2009). Effects of fire on regional evapotranspiration in the central Canadian boreal forest. Global Change Biology, 15(5), 1242–1254. https://doi.org/10.1111/j.1365-2486.2008.01776.x

Brockway, D. G., Gatewood, R. G., & Paris, R. B. (2002a). Restoring fire as an ecological process in shortgrass prairie ecosystems: initial effects of prescribed burning during the dormant and growing seasons. Journal of Environmental Management, 65(2), 135–152. https://doi.org/10.1006/jema.2002.0540

Butler BW, Anderson W, Catchpole EA (2007) Influence of slope on fire spread rate. In 'The Fire Environment – Innovation, Management, and Policy', (Eds BW Butler, W Cook) USDA Forest Service, Rocky Mountain Research Station, pp. 75–83. (Fort Collins, CO).

Chambers, S. D., & Chapin, F. S. (2002). Fire effects on surface-atmosphere energy exchange in Alaskan black spruce ecosystems: Implications for feedbacks to regional climate. Journal of Geophysical Research, 108(D1). https://doi.org/10.1029/2001jd000530

Hess, J. C., Scott, C. A., Hufford, G. L., & Fleming, M. D. (2001). El Niño and its impact on fire weather conditions in Alaska. International Journal of Wildland Fire, 10(1), 1. https://doi.org/10.1071/wf01007

Kennett, D., Kennett, J., West, G., Erlandson, J., Johnson, J., Hendy, I., West, A., Culleton, B., Jones, T., & Staffordjr, T. (2008). Wildfire and abrupt ecosystem disruption on California's Northern Channel Islands at the Ållerød–Younger Dryas boundary (13.0–12.9ka). Quaternary Science Reviews, 27(27–28), 2530–2545. https://doi.org/10.1016/j.quascirev.2008.09.006

Kuljian, H., & Varner, J. M. (2010). The effects of sudden oak death on foliar moisture content and crown fire potential in tanoak. Forest Ecology and Management, 259(10), 2103–2110. https://doi.org/10.1016/j.foreco.2010.02.022

LANDFIRE, Remap 2016, LANDFIRE 2.0.0, U.S. Department of the Interior, Geological Survey.

Li, Jing; Mahalingam, Shankar; Weise, David R. 2016. Chaparral shrub bulk density and fire behavior. Fort Collins, CO: Forest Service Research Data Archive. https://doi.org/10.2737/RDS-2016-0031

Linn Rodman , Reisner Jon , Colman Jonah J. Winterkamp Judith (2002) Studying wildfire behavior using FIRETEC. International Journal of Wildland Fire 11, 233-246. https://doi.org/10.1071/WF02007

Linn Rodman , and F. H. Harlow, 1998, FIRETEC: A transport model for investigating self-determining wildfire. Preprints, Second Symp. on Fire and Forest Meteorology, Phoenix AZ, Amer. Meteor. Soc., 14–19.

Mutlu, M., Popescu, S. C., & Zhao, K. (2008). Sensitivity analysis of fire behavior modeling with LIDAR-derived surface fuel maps. Forest Ecology and Management, 256(3), 289-294.

Neary, D. G., Klopatek, C. C., DeBano, L. F., & Ffolliott, P. F. (1999). Fire effects on belowground sustainability: a review and synthesis. Forest Ecology and Management, 122(1–2), 51–71. https://doi.org/10.1016/s0378-1127(99)00032-8

Pechony, O., & Shindell, D. T. (2010). Driving forces of global wildfires over the past millennium and the forthcoming century. Proceedings of the National Academy of Sciences, 107(45), 19167–19170. https://doi.org/10.1073/pnas.1003669107

Rao, K., Williams, A.P., Fortin, J. & Konings, A.G. (2020). SAR-enhanced mapping of live fuel moisture content. Remote Sens. Environ., 245., https://doi.org/10.1016/j.rse.2020.111797.

Raposo, J. R., Cabiddu, S., Viegas, D. X., Salis, M., & Sharples, J. (2015). Experimental analysis of fire spread across a two-dimensional ridge under wind conditions. International journal of wildland fire, 24(7), 1008-1022.

Raupach, M. R., Finnigan, J. J., & Brunet, Y. (1996). Coherent Eddies and Turbulence in Vegetation Canopies: The Mixing-Layer Analogy. In Boundary-Layer Meteorology 25th Anniversary Volume, 1970–1995 (pp. 351–382). Springer Netherlands. https://doi.org/10.1007/978-94-017-0944-6_15

Reisner, J., Wynne, S., Margolin, L., & Linn, R. R. (2000). Coupled Atmospheric–Fire Modeling Employing the Method of Averages. 793 Monthly Weather Review, 128, 3683–3691.

Scott, Joe H.; Burgan, Robert E. 2005. Standard fire behavior fuel models: a comprehensive set for use with Rothermel's surface fire spread model. Gen. Tech. Rep. RMRS-GTR-153. Fort Collins, CO: U.S. Department of Agriculture, Forest Service, Rocky Mountain Research Station. 72 p.

Sharples, Jason J., Richard HD McRae, and Stephen R. Wilkes. "Wind–terrain effects on the propagation of wildfires in rugged terrain: fire channelling." International Journal of Wildland Fire 21.3 (2012): 282-296.

Sharples JJ, McRae RHD, Wilkes SR (2012) Wind-terrain effects on the propagation of wildfires in rugged terrain: Fire channelling. International Journal of Wildland Fire 21, 282–296. doi:10.1071/WF10055

Sullivan, A. L. (2009). Wildland surface fire spread modelling, 1990 - 2007. 1: Physical and quasi-physical models. International Journal of Wildland Fire, 18(4), 349. https://doi.org/10.1071/wf06143

Swetnam, T. W. (1993). Fire History and Climate Change in Giant Sequoia Groves. Science, 262(5135), 885–889. https://doi.org/10.1126/science.262.5135.885

U.S. Geological Survey, 2019, The National Map—New data delivery homepage, advanced viewer, lidar visualization: US. Geological Survey Fact Sheet 2019–3032, 2 p., https://doi.org/10.3133/fs20193032

van der Werf, G. R., Randerson, J. T., Giglio, L., Collatz, G. J., Mu, M., Kasibhatla, P. S., Morton, D. C., DeFries, R. S., Jin, Y., & van Leeuwen, T. T. (2010). Global fire emissions and the contribution of deforestation, savanna, forest, agricultural, and peat fires (1997–2009). Atmospheric Chemistry and Physics, 10(23), 11707–11735. https://doi.org/10.5194/acp-10-11707-2010